Isr. J. Earth Sci.; 48: 257–264

Deformation along the margins of the Dead Sea Transform: The Yehudiyya Block, Golan Heights

Shaul Hurwitz,[a] Ari Matmon,[a,b,*] Hagai Ron,[c] and Ariel Heimann[b]
[a]Institute of Earth Sciences, The Hebrew University of Jerusalem, Jerusalem 91904, Israel
[b]Geological Survey of Israel, 30 Malkhe Yisrael Street, Jerusalem 95501, Israel
[c]The Geophysical Institute of Israel, P.O. Box 182, Lod 71100, Israel

(Received 14 December 1999; accepted 1 February 2000)

ABSTRACT

Hurwitz, S., Matmon, A., Hagai, R., Heimann, A. 1999. Deformation along the margins of the Dead Sea Transform: The Yehudiyya Block, Golan Heights. Isr. J. Earth Sci. 48: 257–264.

The Yehudiyya Block (YB) is located in the western part of the Golan Heights, along the eastern margins of the Dead Sea Transform. The block, covered by basalt, is part of the unfaulted plateau of the Golan Heights and dips to the southwest towards the Beteiha Valley and the shores of the Sea of Galilee. A set of NNW-trending normal faults traverses the YB and dissects the basalt. K–Ar dating and paleomagnetic analysis were applied to examine the history of faulting in the YB. Thirty-three basalt flows from five locations were sampled for paleomagnetic analysis, and eight samples were sampled for K–Ar age dating. The age of the basalt ranges between 2.19 ± 0.06 and 0.41 ± 0.24 Ma. The mean measured declination and inclination in the YB are $0.6° \pm 5.2°$ and $46.4° \pm 4.6°$, respectively. This indicates that deformation was not accompanied by block rotation. It is suggested that tilting of the entire YB and faulting within the block occurred in response to a major subsidence event in the adjacent Kinnarot Basin that commenced approximately 1 m.y. ago. Faulting has caused a maximum extension of 0.6% to 1.3% in a NNE–SSW direction.

INTRODUCTION

The Dead Sea Transform (DST) extends over 1,000 km between the Red Sea spreading zone and the Alpine convergent zone in southern Turkey (Fig. 1a). It separates the Sinai sub-plate to the west from the Arabian plate to the east. Left lateral displacement of 105 km has occurred along the southern part of the DST since its formation in the Middle Miocene (Freund et al., 1970; Garfunkel, 1981).

In the central strand of the DST, deformation along its western margins (Sinai sub-plate) is complex and accommodated by slip oblique to the trend of the transform (Freund, 1970). In contrast, oblique faulting is less abundant along the eastern margins (Arabian plate). The Golan Heights on the eastern margins of the transform are mostly unfaulted. An exception is the Yehudiyya Block (YB; also named Meshushim Block), located in the western part of the Golan

*Author to whom correspondence should be addressed.
E-mail: matmon@tx.technion.ac.il

© 1999 Laser Pages Publishing Ltd. 0021-2164/99 $4.00

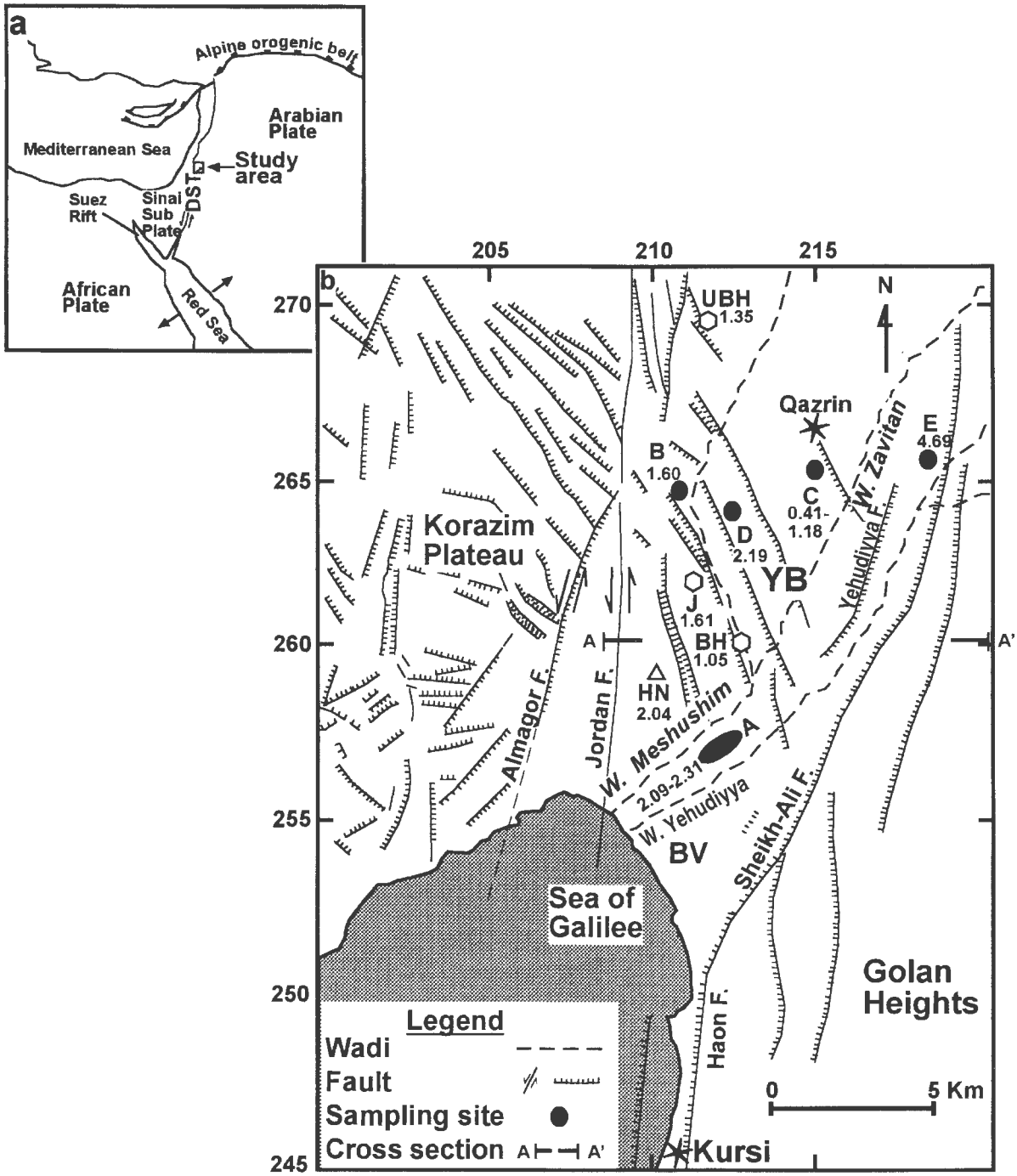

Fig. 1. (a) Map showing the general tectonic setting of the Dead Sea Transform (DST). (b) Location map (on Israel grid) showing the main faults in the Yehudiyya Block (YB) and adjacent areas (after Michelson, 1979; Mor, 1986; Belitzky, 1987; Heimann, 1990). Sampling sites for dating and paleomagnetism: A—Yehudiyya road (2120/2573), B—Wadi Meshushim (2101/2638), C—Wadi Sheikh Mussa (2137/2653), D—Wadi Asaliya (2129/2635), and E—Qazbia Junction (2172/2652). Numbers are K–Ar averaged ages of the basalt sequence at each sampling location. Open hexagons—sampling locations and K–Ar ages from Mor (1986): BH—Meshushim Pool, J—Jerba, UBH—Upper Bet Hameches. Open triangle—sampling location and K–Ar dating from Heimann (1990): Had-Nes (HN). A–A′ is the location of the cross section in Fig. 2. BV—Beteiha Valley.

Heights, to the east of the DST (Fig. 1b). The basaltic cover of this domain is traversed by a set of normal faults striking to the NNW (Michelson, 1979; Mor, 1986; Heimann, 1990). The strike of theses faults is different from the strike of the faults which traverse the adjacent Korazim Plateau (Belitzky, 1987; Heimann and Ron, 1993) on the western side of the Jordan fault (Fig. 1b).

In this study, we incorporate K–Ar dating to examine the temporal framework of faulting and paleomagnetic analysis to determine the style of deformation in the YB. The results emphasize the different modes of deformation along the margins of the DST.

STUDY AREA

The YB, located on the western margins of the Golan Heights, is approximately 150 km^2 in size. It is covered by Upper Pliocene to Pleistocene basalt (Mor, 1986; Weinstein et al., 1994; Heimann et al., 1996). The block is confined by the Jordan Fault (a segment of the DST) in the west, the SW–NE-trending Sheikh-Ali Fault in the east and NE (Michelson, 1979; Rotstein and Bartov, 1989; Sneh et al., 1998), and by the Sea of Galilee in the SW (Fig. 1). There is no tectonic separation between the YB and the volcanic plateau of the Golan Heights in the NE. The YB dips to the southwest from an elevation of approximately 300 m above msl (near the town of Qazrin) to 200 m below msl at the Sea of Galilee, a distance of approximately 13 km.

The YB is traversed by a parallel set of NNW-trending normal faults (Michelson, 1979; Mor, 1986; Heimann, 1990) (Fig. 1b). These faults, spaced by 1,200–1,500 m, are 3 to 5 km in length and are nearly perpendicular to the Sheikh-Ali Fault (Fig. 1b). These faults bound a series of tilted blocks and small horsts and grabens with a clear topographic expression (Fig. 2). Normal displacement generally does not exceed 40 m on each individual fault (Michelson, 1979; Mor, 1986; Heimann, 1990).

Faulting within the YB was accompanied by normal faulting along the Sheikh-Ali Fault (Mor, 1986; Heimann, 1990). Vertical displacement along this fault commenced prior to the faulting within the YB in the Lower Pleistocene. This is indicated by the occurrence of Pleistocene basalt north of the Sheikh-Ali Fault, but the absence of coeval basalt south of the fault (Heimann, 1990; Sneh et al., 1998). The Jordan Fault, separating the YB from the Korazim Plateau (Fig. 1), is currently active, as indicated by historical and instrumental recorded earthquakes (van Eck and Hofstetter, 1990; Ben-Menahem, 1991; Ellenblum et al., 1998).

The Beteiha (Bet Zeida) Valley in the southwestern part of the YB is located between the en echelon Jordan and Haon faults (Fig. 1). The valley hosts a sequence of alluvial deposits discharged by some of the major rivers flowing from the Golan Heights into the Sea of Galilee. The absence of a pronounced Bouguer gravity anomaly in the Beteiha Valley (Ben-Avraham et al., 1996) suggests that the basin is not deep.

The Korazim Plateau (Fig. 1), on the western side of the DST, was deformed extensively during the Pleistocene, as indicated by morphological escarpments (Belitzky, 1987) and by 11.4° ± 4.0° counterclockwise block rotation along the faults that cross the plateau (Heimann and Ron, 1993).

METHODS

K–Ar dating

Eight samples from four different locations were sampled for K–Ar age dating (sites A to D in Fig. 1b). The samples were collected from the base and top of the sequences. In one case, where a magnetic reversal

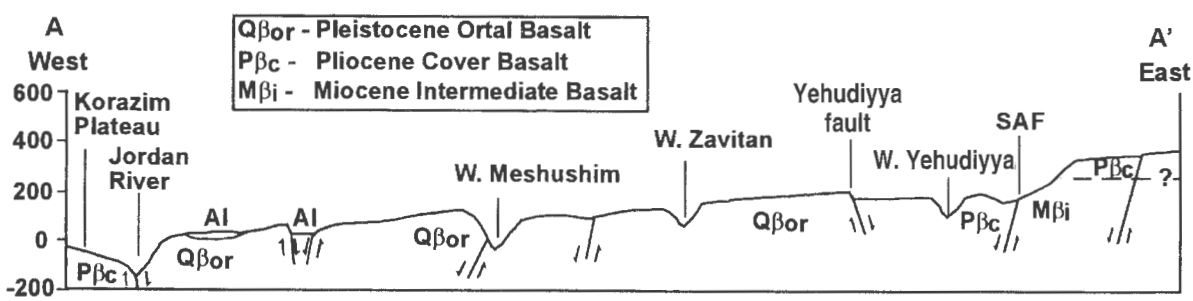

Fig. 2. Cross section of the Yehudiyya Block depicting the general dip of the block and the major faults (modified after Mor, 1986).

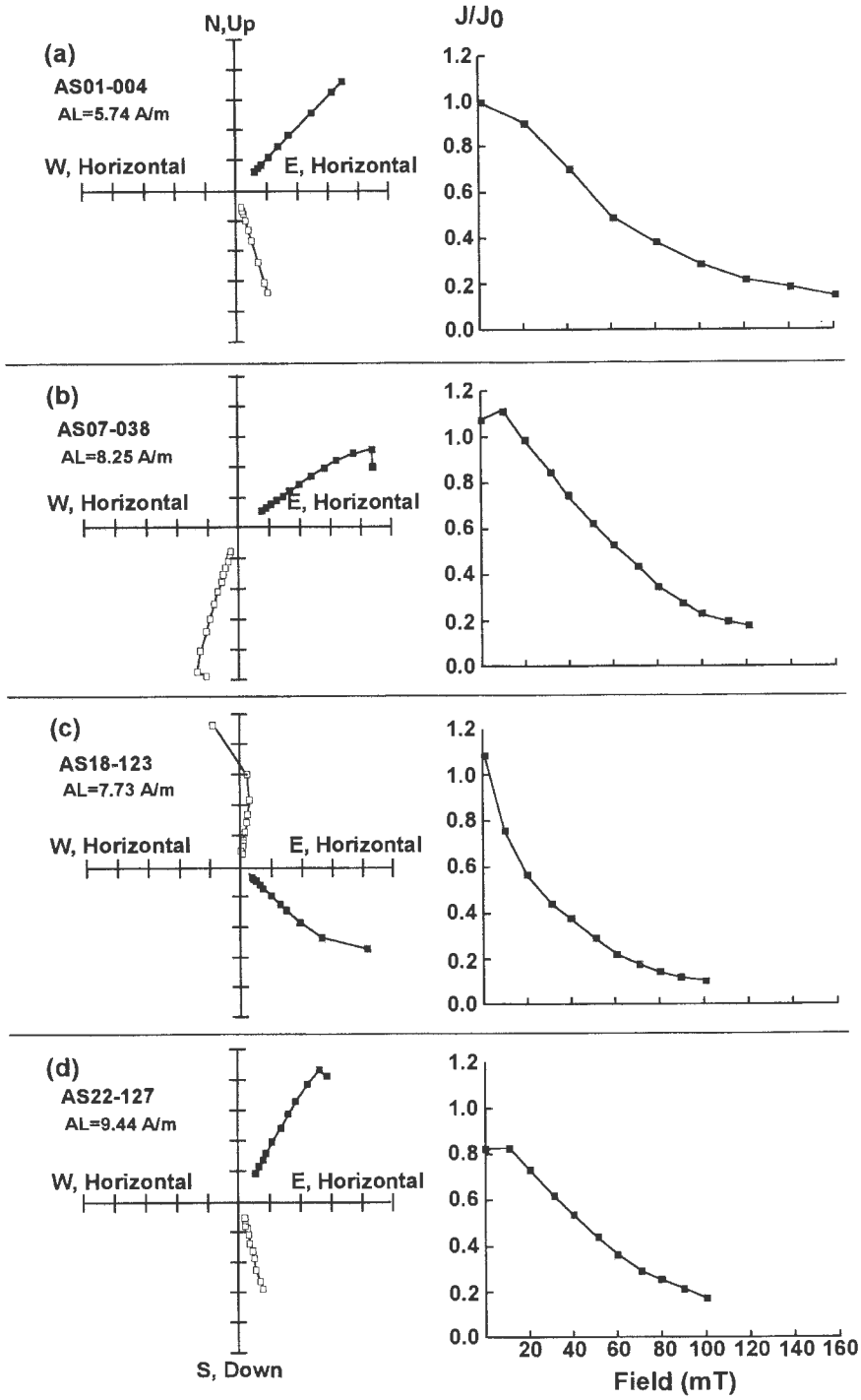

Fig. 3. Demagnetization sequence of four typical samples: a, b, c, d from sites A, B, C, and D, respectively (see Table 1). Within each figure, orthogonal demagnetization diagrams of declination and true inclination are plotted on the left-hand side and normalized intensity plots are on the right-hand side. For the declination plot the vertical axis corresponds to geographic N–S and the horizontal axis to geographic E–W. Axis lengths are given in SI units. For the true inclination plots, the vertical axis is the up–down direction and the horizontal axis is parallel to a plane containing the true inclination. Normalized intensity plot shows the demagnetization level versus the normalized intensity (J/J_0).

was found within a sequence (Site C), an additional sample was collected from within the sequence. A short description of the experimental procedures is given below. More detailed descriptions are to be found in Heimann (1990), Heimann et al. (1992), and Heimann and Ron (1993). Samples, of ~1 kg were crushed and sieved (70–90 mesh; 212–170 μm); washed with water, alcohol, and acetone; and leached with 0.5 N HCl for 1 h. Final cleaning of the samples was carried out by magnetic separation. Potassium was measured by atomic absorption and ^{40}Ar by isotope dilution. Argon was analyzed on a VG MM1200B mass spectrometer at the Geological Survey of Israel Geochronological Laboratory. The constants used are according to IUGS (Steiger and Jäger, 1977).

Paleomagnetism

Thirty-three basalt flows from five locations (sites A to E in Fig. 1b) on different tectonic blocks within the YB were sampled for paleomagnetic analysis. Samples were collected as oriented, field-drilled, one-inch cores. Sites were selected so that they cover the time span represented by the basalt flows in the YB and geographically cover the domain. Typically, six cores from each basalt flow were collected. All sampled basalt flows are horizontal to sub-horizontal. Cores were sliced into 2.5-cm-long cylinders for routine paleomagnetic measurement. Natural remanant magnetization (NRM) of all samples was made using a three-axis 2G 750™ superconducting magnetometer with integrated alternating field (AF) coils. The lowest remanant signal that can be measured by the cryogenic magnetometer is 10^{-6} A/m, and the maximum alternating field (AF) produced by the coil is 200 mT. The samples were stepwise demagnetized in an AF up to a maximum of 160 mT by increments of 10 or 20 mT (Fig. 3). This procedure removed about 90% of the magnetization. All samples except from one site show a stable single vector with high to moderate coercivity typical of a signal of pseudo-single titanomag-netite. A soft present-field overprint was present in a few cases. In order to assess the magnetic behavior and stability of the samples, orthogonal vector plots and normalized intensity(J/J_0) curves were plotted (Fig. 3). The samples showed initial NRM intensity (J_0) of 10^{-1} A/m. The magnetization component directions were derived using a three-dimensional least-squares method (Kirschvink, 1980). The direction of magnetization for all samples is presented on a stereonet plot (Fig. 4).

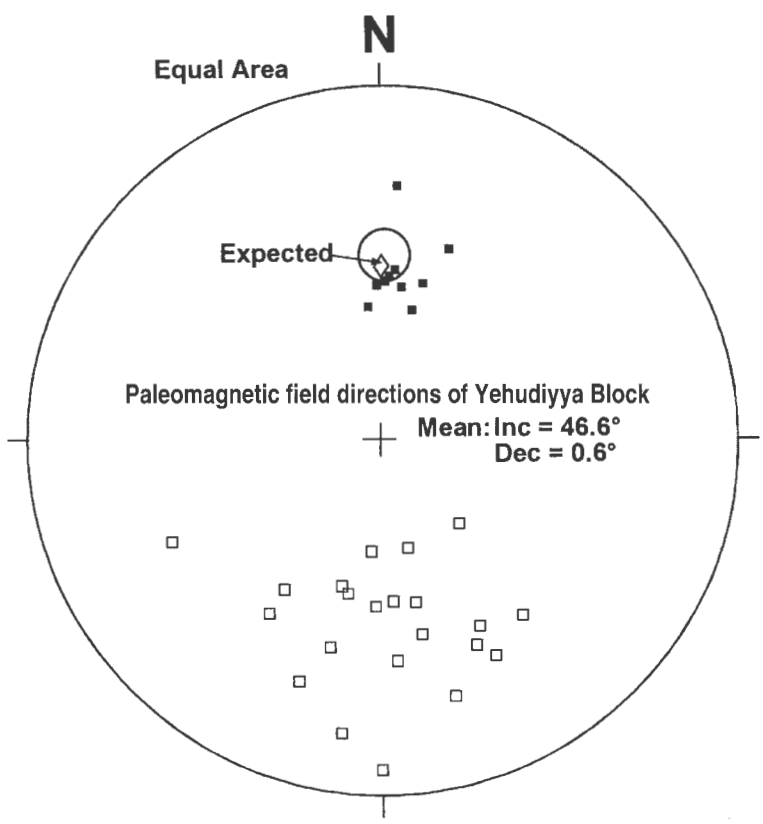

Fig. 4. Upper hemisphere equal-area projection of site mean paleomagnetic vectors. Solid squares are positive inclination and open squares are negative inclination. Each square represents the average of a single site. The small circle is the 95% confidence area about the mean. The open diamond in the lower part of the small circle is the expected Pliocene–Pleistocene magnetic field of the Arabian plate (from Besse and Courtillot, 1991).

Table 1. Paleomagnetic and K–Ar dating results

Site	Location	DEC	INC	k	α_{95}	n	Polarity	Age (Ma)*
AS01	A	167.7	–43.3	183.7	4.6	5	R	2.31 ± 0.08(3)
AS02	A	176.3	–36.7	86.8	6.1	6	R	
AS03	A	192.3	–52.9	54.9	7.7	6	R	
AS04	A	182.5	–50.8	70.4	6.8	6	R	
AS05	A	176.4	–51.6	23.0	6.8	5	R	2.09 ± 0.08(3)
AS06	B	199.3	–54.4	178.8	4.3	6	R	1.60 ± 0.17(2)
AS07	B	212.8	–48.0	53.8	8.5	5	R	
AS08	B	198.9	–27.6	34.3	9.8	6	R	
AS09	B	188.1	–17.4	478.1	3.7	3	R	
AS10	B	212.6	–41.0	70.8	7.4	5	R	
AS11	B	194.5	–38.6	31.2	11.2	5	R	
AS12	B	136.6	–62.6	2.7	11.8	4	R	
AS13	B	244.1	–34.0	26.3	115.8	3	**	1.59 ± 0.07(2)
AS14	C	179.5	–6.9	22.4	14.8	4	R	1.18 ± 0.12(3)
AS15	C	4.0	29.1	70.9	7.4	5	N	0.54 ± 0.42(2)
AS16	C	13.5	59.2	148.0	5.8	4	N	
AS17	C	16.3	52.2	152.3	5.1	5	N	
AS18	C	8.2	54.0	75.2	6.6	6	N	
AS19	C	20.0	42.0	81.5	6.3	6	N	
AS20	C	354.8	59.2	45.7	8.5	6	N	0.41 ± 0.24(2)
AS21	D	192.0	28.2	31.2	11.2	6	**	
AS22	D	185.1	–64.3	57.7	10.6	3	R	
AS23	D	166.2	–63.7	144.0	4.8	6	R	
AS24	D	168.4	–51.3	36.7	10.3	5	R	
AS25	D	154.7	–36.5	199.0	4.4	5	R	
AS26	D	151.6	–39.9	77.5	6.5	6	R	
AS27	D	140.6	–35.7	24.6	11.5	6	R	
AS28	D	151.5	–31.4	21.9	12.2	6	R	
AS29	D	164.2	–24.9	17.5	13.7	6	R	2.19 ± 0.06(2)
KZ1	E	2.9	52.2	258.3	3.6	6	N	
KZ2	E	2.0	53.4	167.2	4.4	6	N	
KZ3	E	359.3	54.1	273.3	3.5	6	N	
KZ4	E	4.9	50.2	557.6	2.4	6	N	4.69 ± 0.30(3)
Mean of sites		0.6	46.4	18.6	5.8	31		

The different locationlocations of sampling are presented in Fig. 1. A—Yehudiyya road, B—Wadi Meshushim, C—Wadi Sheikh Mussa, D—Wadi Asaliya, E—Qazbia Junction. k is a precision parameter; α_{95} is radius of 95% confidence in degrees. The number in the parenthesis near the age is the number of K–Ar measurements of the same sample. Within each location, the sites are in order from the base to the top. *Detailed analytical data of the K–Ar method can be obtained from A.H. **Sites excluded from the analysis.

RESULTS

The K–Ar ages of the selected samples are presented in Table 1 and Fig. 1. The dated samples from the YB represent the time range between 2.19 ± 0.06 and 0.41 ± 0.24 Ma, in accordance with previous measurements (Mor, 1986; Heimann, 1990; Fig. 1). The age of the basalt from the Qazbia Junction (Location E in Table 1) is 4.69 ± 0.30 (Heimann, unpublished data) and is classified as Cover Basalt (Heimann et al., 1996). Where both the base of the sampling location and its top were sampled, the age of the base was always older, as expected (Table 1).

The results of the paleomagnetic analysis are presented in Table 1 and Fig. 4. Most samples show a characteristic stable vector, mostly single component. All samples from sites AS13 and AS21 exhibited unstable behavior, and therefore were excluded from further analysis. Mean paleomagnetic directions for each site and the mean direction for the entire YB domain were calculated using the Fisher (1953) statistical method.

The mean direction of the 31 sites in the YB is Dec = 0.6° ± 5.2° and Inc = 46.4° ± 4.6°. According to

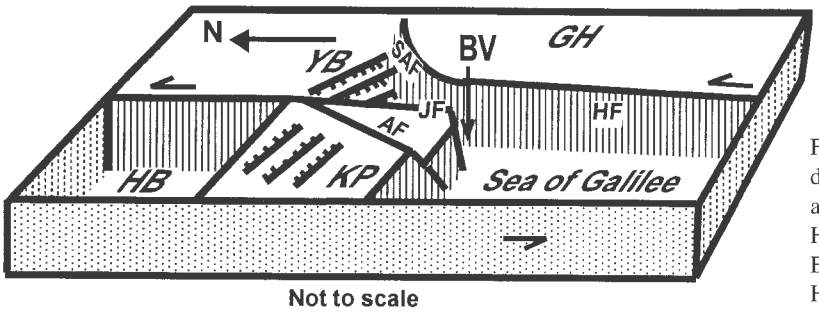

Fig. 5. A conceptual, not to scale, block diagram of the study area showing tilting and normal faulting within the YB. HB—Hula Basin, YB—Yehudiyya Block, SAF—Sheikh Ali Fault, HF—Haon Fault, AF—Almagor Fault, JF—Jordan Fault, BV—Beteiha Valley, KP—Korazim Plateau, GH—Golan Heights.

statistical criteria (Demarest, 1983), this indicates that there was no significant rotation when comparing to the expected Plio-Pleistocene magnetic field direction of this region, Dec = 0°; Inc = 52.4°, as calculated from Besse and Courtillot (1991). The averaging of secular variations of the geomagnetic field is evidenced by the Fisherian distribution, the k value (precision parameter), and the relatively low α_{95}, the dual polarity population, and the time span represented by the samples (Table 1). In 21 out of the 31 measured sites, the paleomagnetic polarity was reverse. The transition from reverse to normal (flow AS14 and AS15) represents a noncontinuous record and not a real field transition, as evident from the age of the two flows (Table 1).

DISCUSSION AND CONCLUSIONS

Previous geological mapping indicates that the set of NNW-trending striking normal faults in the YB displace basalts covering the YB (Michelson, 1979; Mor, 1986; Heimann, 1990). K–Ar dating implies that the age range of these basalts is between 2.31 ± 0.08 and 0.41 ± 0.24 Ma. The youngest dated basalt was sampled in Wadi Sheikh Mussa (location C in Fig. 1b), adjacent to an exposed fault, and therefore it is concluded that at least part of the faulting in the YB has occurred post 400 Ka. Previous paleomagnetic studies along the margins of the DST in northern Israel indicate variable amounts of block rotation in different tectonic domains during the Pliocene to Pleistocene (Ron, 1984; Ron et al., 1990; Heimann and Ron, 1993). Paleomagnetic analysis results from this study indicate that in the YB faulting was not accompanied by significant block rotation. Different modes of deformation exist in the Korazim Plateau and the YB. While tectonic blocks within the Korazim Plateau were rotated 11.4° counterclockwise since 0.8–0.9 Ma, blocks in the YB were not rotated in the last 2 Ma. This suggests that the local stress field along the margins of the DST is complex. Thus, deformation along the margins of the transform in the region is dominated by local stress fields rather than by the expected regional stress field of the DST (σ_1~330°) (Eyal and Reches and Eyal, 1983; Eyal, 1996).

The maximum amount of extension across the 13 km of the YB in a NNE–SSW direction can be calculated assuming that there are 7 normal faults in the YB, that the vertical displacement on each of the faults is 40 m (Michelson, 1979; Mor, 1986; Heimmann, 1990), and that the dip of all faults is 60°. Taking these assumptions into account, the amount of lateral displacement on each fault is 23 m and the total extension is 1.3%.

It is suggested here that normal faulting within the YB, accompanied by development of tectonic blocks that step downwards to the southwest and the tilting of the entire block, probably occurred in response to a major subsidence event in the Kinnarot Basin (Ben-Gai and Reznikov, 1997; Fig. 5). This event commenced approximately 1 m.y. ago (Heimann, 1990) and formed a deep depression offshore at Kursi, on the eastern margins of the Sea of Galilee (Ben-Gai and Reznikov, 1997; Fig. 1b).

ACKNOWLEDGMENTS

We thank Ronit Kessel for helping us in the field and Carmel Dallal for technical assistance in the Geochronological Laboratory. Meir Abelson and Amotz Agnon are thanked for their reviews.

REFERENCES

Belitzky, S. 1987. Tectonics of the Korazim Saddle. M.Sc. thesis, Hebrew Univ., Jerusalem, 94 pp. (in Hebrew, English abstr.).

Ben-Avraham, A., ten-Brink, U., Bell, R., Reznikov, M.

1996. Gravity field over the Sea of Galilee: Evidence for a composite basin along a transform fault. J. Geophys. Res. 101: 533–544.

Besse, J., Courtillot, V. 1991. Revised and synthetic apparent polar wander paths of the African, Eurasian, North American and Indian Plates, and true polar wander since 200 Ma. J. Geophys. Res. 96: 4029–4050.

Ben-Gai. Y., Reznikov, M. 1997. A multi-channel seismic survey in Lake Kinneret. Rep. 733/16/97, Geophys. Inst. Israel, Lod, 12 pp.

Ben-Menahem, A. 1991. Four thousand years of seismicity along the Dead Sea Rift. J. Geophys. Res. 96: 20195–20216.

Demarest, H.H. 1983. Error analysis for the determination of tectonic rotation from paleomagnetic data. J. Geophys. Res. 88: 4321–4328.

Ellenblum, R., Marco, S., Agnon, A., Rockwell, T., Boas, A. 1998. Crusader castle torn apart by earthquake at dawn, 20 May 1202. Geology 26: 303–306, 1998.

Eyal, Y. 1996. Stress field fluctuations since the middle Miocene. Tectonics 15: 157–170.

Eyal, Y., Reches, Z. 1983. Tectonic analysis of the Dead Sea Rift region since the late Cretaceous based on mesostructures. Tectonics 2: 167–185.

Fisher, R.A. 1953. Dispersion on a sphere. Proc. R. Soc. London, A217: 295–305.

Freund, R. 1970. The geometry of faulting in the Galilee. Isr. J. Earth Sci. 19: 117–140.

Freund, R., Garfunkel, Z., Zak, I., Goldberg, T., Weissbrod, T., Derin, B. 1970. The shear along the Dead Sea Rift. Philos. Trans. R. Soc. London 267: 107–130.

Garfunkel, Z. 1981. Internal structure of the Dead Sea leaky transform (rift) in relation to plate kinematics. Tectonophysics 80: 81–108.

Heimannn, A. 1990. The development of the Dead Sea Rift and its margins in northern Israel during the Pliocene and Pleistocene. Ph.D. thesis, Hebrew Univ., Jerusalem, 82 pp. (in Hebrew, English abstr.).

Heimannn, A., Ron, H. 1993. Geometrical changes of plate boundaries along part of the northern Dead Sea Transform: geochronologic and paleomagnetic changes. Tectonics 12: 477–491.

Heimannn, A., Steinitz, G., Mor, D., Shaliv, G. 1996. The Cover Basalt formation, its age and its regional and tectonic setting: implications from K–Ar and $^{40}Ar/^{39}Ar$ geochronology. Isr. J. Earth Sci. 45: 55–71.

Kirscvink, J.L. 1980. The least-square line and plane and the analysis of paleomagnetic data. Geophys. J. R. Astron. Soc. 26: 669–718.

Michelson, H. 1979. The geology and paleogeogrophy of the Golan Heights. Ph.D. thesis, Tel Aviv University, 163 pp. (in Hebrew, English abstr.).

Mor, D. 1986. The volcanism of the Golan Heights. Ph.D. thesis, Geol. Surv. Isr. Rep. GSI/5/86, Hebrew Univ., Jerusalem, 159 pp. (in Hebrew, English abstr.).

Ron, H., Freund, R., Garfunkel, Z., Nur., A. 1984. Block rotation by strike slip faulting: structural and paleomagnetic evidence. J. Geophys. Res. 89: 6256–6270.

Rotstein, Y., Bartov, Y. 1989. Seismic reflection across a convergent continental transform: an example from the Dead Sea rift in Northern Israel. J. Geophys. Res. 94: 2902–2912.

Sneh, A., Lang, B., Halicz, L. 1998. The Sheikh Ali fault, NE Lake Kinneret, implications of new volcano-stratigraphic findings. Geol. Surv. Isr. Current Research 11: 42–44.

Steiger, R.H., Jäger, E. 1977. Subcommission on geochronology: Convention on the use of decay constants in geochronology and cosmochronology. Earth Planet. Sci. Lett. 36: 359–362.

van Eck, T., Hofstetter, A. 1990. Fault geometry and spatial clustering of microearthquakes along the Dead Sea-Jordan rift fault zone. Tectonophysics 180: 15–27.

Weinstein, Y., Navon, O., Lang, B. 1994. Fractionation of Pleistocene alkali-basalts from the northern Golan Heights, Israel. Isr. J. Earth Sci. 43: 63–79.